





## CONTENTS

1. INTRODUCTION .....	1
2. POWERED ROCKET ASCENT NEGLECTING EARTH'S ROTATION EFFECTS .....	2
The Equations of Motion .....	2
Integrations of the Equations of Motion .....	6
3. INCLUSION OF EARTH'S ROTATION .....	7
4. ORBIT TRAJECTORY FROM INJECTION CONDITIONS AT ROCKET BURNOUT .....	16
5. VEHICLE FLIGHT SEEN BY INERTIAL AND EARTH OBSERVERS .....	20
6. DISCUSSION .....	21
7. ACKNOWLEDGMENTS .....	22
8. REFERENCES .....	22
APPENDIX A – Lagrangian Method, Including the Presence of Nonconservative Forces .....	23
APPENDIX B – Derivation of the Lagrangian and Generalized Forces for the Rocket Problem .....	25
APPENDIX C – Velocity Increment Estimates for Various Effects in First-Stage Rocket Motion .....	27
APPENDIX D – Determination of Launch Profile Parameters from Desired Orbit Injection Conditions in a Flat Earth Approximation .....	28
APPENDIX E – Thrust Increase and Aerodynamic Effects .....	30



# EQUATIONS OF POWERED ROCKET ASCENT AND ORBIT TRAJECTORY

## 1. INTRODUCTION

In the analysis of systems in space, one often encounters the problem of specification and design of a launch vehicle and its trajectory, so that certain performance requirements may be met. Also of interest are the flight path of the space vehicle in orbit, particularly with respect to interactive ground systems, and the relation of the orbit to the launch profile. As will be explained below, however, it is usually difficult to extract the requisite information from various standard references. This report should help to remedy this situation. One of the primary goals of this report is to present a logical exposition of approximations and sufficient information and guidance to facilitate an investigator's choice of the simplest analysis technique suited to his needs. He may thus possibly be able to avoid an unnecessarily complex, time-consuming analysis technique, such as the "full" numerical solution approach to the problem.

In many standard reference sources on powered rocket ascent from the earth, equations are introduced in an ad hoc and incomplete manner. There are also inaccuracies and inconsistencies to contend with. For example, Ball and Osborne's Eqs. (1-20) and (1-22) [1] leave out certain kinematic terms which are related to a radial gravitational field and could become important for high rocket velocities. Ehrlicke [2] correctly introduces the effect of these terms in his Eq. (5-27) in an ad hoc fashion, but then he seemingly *incorrectly* introduces their effect later in his Eqs. (6-39) and (6-40), also in an ad hoc fashion. Ruppe [3] gives a basically correct treatment of these terms in his Eqs. (3.1)-(3.4), but from the outset his treatment ignores the orientation or angle of attack of the vehicle through his use of a gravity tilt condition. Furthermore, Ball and Osborne [1] give a sketchy treatment of earth's rotation effects, in which an initial rocket velocity imparted by earth's rotation is included in a flat earth approximation. Ruppe [3] does a more complete job on this, but his results are also restricted to a flat earth. In most instances a powered rocket ascent will not cover a large enough ground range to necessitate taking curvature of the earth into account, but in some cases it will. To cover these cases, where ground range might be in excess of 500 n.mi., a correct treatment of earth's curvature effects is necessary, but it is absent from the references that have been discussed [1-3].

This report is intended to remedy the above deficiencies and present in one place, in a consistent notation set, and in reasonably coherent fashion the basic equations of powered rocket ascent and orbit trajectory needed for analysis techniques at various levels of approximation. To start with, in the first part of Section 2, we obtain the rocket equations of motion in an inertial frame. As in nearly all elementary treatments, the complications from the fact that the atmosphere is not stationary in an inertial reference frame are initially ignored. In the latter part of this section these equations of motion are integrated to give velocity and coordinate expressions as a function of time in an inertial frame. In Section 3, we consider the complications of

earth's rotation, including the effect of a corotating atmosphere. A "full" solution of the rocket trajectory would thus involve a complicated three-dimensional numerical solution of the equations of motion. In Section 3 it is shown that the great complications which arise from this course of action can be avoided by solving simplified equations of motion in the earth-fixed, rotating reference frame for the period of powered rocket ascent when aerodynamic effects are important; the data are then transformed back to the inertial frame, which amounts to addition of a rotation velocity vector; and finally the inertial velocities computed as in Section 2 for portions of the rocket flight when aerodynamic effects are not important are added. The results of Section 3 demonstrate that approximate velocity and coordinate expressions for rocket flight can be obtained by a rather simple extension of results from Section 2. The expressions in Section 3 will be found to include, to a good approximation, not only earth and atmosphere rotation effects, but also earth's curvature effects for the total powered trajectory. In Section 4 the nature of the elliptical satellite orbit and its point of entry, as determined from the injection conditions which exist at cutoff of the rocket engines, are considered. In Section 5 the procedures are described for determining the vehicle flight coordinates versus time in both powered and orbital phases, and as seen by both inertial and earth observers. In Section 6 there is a discussion of the equations obtained and their underlying validity.

## 2. POWERED ROCKET ASCENT NEGLECTING EARTH'S ROTATION EFFECTS

### The Equations of Motion

The coordinate system used to describe rocket motion is shown in Fig. 1. The forces on the rocket are the thrust force of the engine, gravity, and aerodynamic forces. As in most elementary treatments [1-3], we assume initially that the atmosphere is stationary, so that aerodynamic forces on the rocket arise purely because of the rocket motion. Actually, the atmosphere corotates with the earth to a first approximation, but for large launch vehicles this turns out to have consequences of only secondary importance for rocket motion [3]. We do, however, include this as one of the rotating earth effects in Section 3. With the assumption of a stationary atmosphere and an axially symmetric rocket in our inertial frame, the simplest case of rocket motion will be planar and conveniently describable in circular coordinates (see Fig. 1), because of the radial nature of the gravitational field and the spherical earth. The effects of earth's rotation will be disregarded for now, but will be included in Section 3. Shown in Fig. 1 are the radius vector  $r$  from the center of the earth to the satellite, its associated altitude  $y$ , the angular displacement from launch  $\phi$ , which gives the ground range  $x$  when the radius of the earth  $R$  is factored in, the flight path angle of the center of mass of the rocket  $\psi$  with respect to the local horizontal (or "heading"), and the angle of attack  $\alpha$  of the rocket axis with respect to the flight direction.

For  $\alpha = 0$  in Fig. 1 the only aerodynamic force on the symmetric rocket will be a drag force opposite to the flight direction. If one defines drag  $D$  and lift  $L$  aerodynamic forces for  $\alpha \neq 0$  as being antiparallel and perpendicular to the flight direction, it is found for small  $\alpha$  that  $L$  is linearly proportional to  $\alpha$  and that the correction to  $D$  is approximately quadratic in  $\alpha$  [2]. Unlike Ehricke [2] and Ruppe [3], Ball and Osborne [1] unconventionally refer drag and lift direction to the rocket axis of symmetry (or "roll" axis). In Fig. 2 we indicate a force diagram for the rocket and include a brief description of the symbols. We use the standard assumptions found in many references [1-3]:

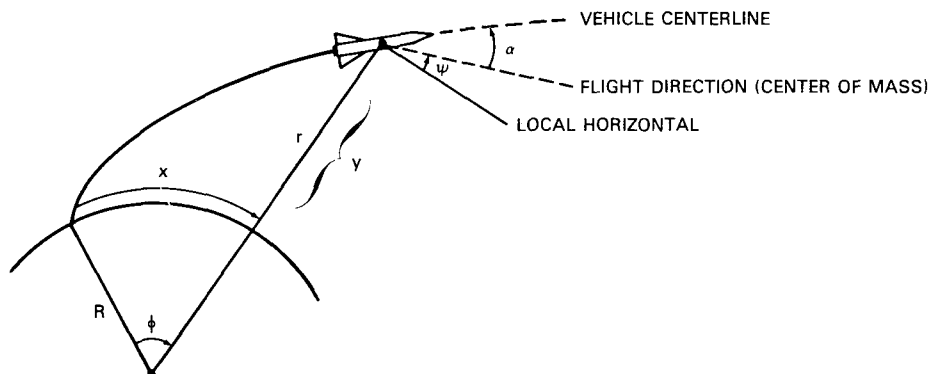
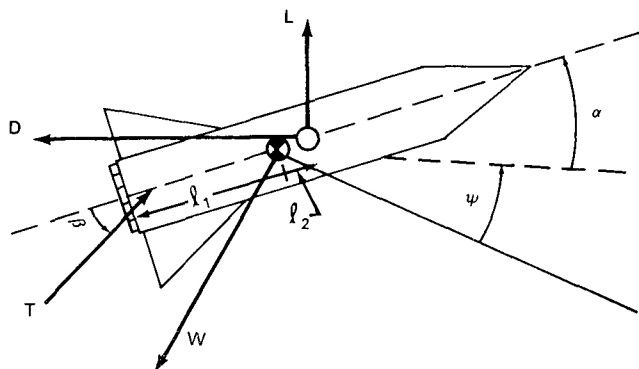


Fig. 1 — Coordinate system for two-dimensional rocket motion



- |                              |   |
|------------------------------|---|
| ● — CENTER OF GRAVITY        | L — LIFT  |
| ○ — CENTER OF PRESSURE       | W — WEIGHT  |
| $\psi$ — FLIGHT PATH HEADING | $l_1$ — VECTOR FROM CENTER OF GRAVITY TO CENTER OF COMBUSTION |
| $\alpha$ — ANGLE OF ATTACK   | $l_2$ — VECTOR FROM CENTER OF GRAVITY TO CENTER OF PRESSURE   |
| T — THRUST FORCE             |   |
| $\beta$ — ANGLE OF THRUST    |   |
| D — DRAG                     |   |

Fig. 2 — Force diagram for the rocket with symbol legend

- the aerodynamic forces act through the center of pressure,
- the force of gravity acts through the center of gravity, and
- the thrust force is applied through the "center of combustion".

One may utilize the Lagrangian method in this problem, suitably generalized to include the presence of nonconservative forces [4]. A brief review of this approach is included in Appendix A. In Appendix B this method is applied to the present problem in finding the Lagrangian L and generalized nonconservative forces.

Lagrange's equations are found as

$$\frac{d}{dt} \frac{\partial L}{\partial \dot{q}_j} - \frac{\partial L}{\partial q_j} = F_{q_j}, \quad (1)$$

where  $q_j = r, \phi,$  and  $\alpha$  in turn. Their evaluation yields

$$\ddot{r} - r\dot{\phi}^2 + K/r^2 = (L/M) \cos \psi - (D/M) \sin \psi + (T/M) \sin (\psi + \alpha + \beta), \quad (2)$$

$$r\ddot{\phi} + 2\dot{r}\dot{\phi} = - (L/M) \sin \psi - (D/M) \cos \psi + (T/M) \cos (\psi + \alpha + \beta), \text{ and} \quad (3)$$

$$I\ddot{\alpha} = I_2[L \cos \alpha + D \sin \alpha] - I_1 T \sin \beta. \quad (4)$$

In effect, Ball and Osborne [1] leave out the term  $r\dot{\phi}^2$  in Eq. (2) and a term  $\dot{r}\dot{\phi}$  in Eq. (3) in their Eqs. (1-20) and (1-22). (Note that  $\dot{r}, r\dot{\theta}$  correspond to their  $\dot{y}, \dot{x}$ ). Equations (2) and (3) are the equations of motion for the radial and angular coordinates of the center of mass, and Eq. (4) applies to the coordinate  $\alpha$  for the internal motion (cf. Fig. 1). The center of mass Eqs., (2) and (3), in which we are particularly interested, can be manipulated as follows.

We have for the velocity of the center of mass:

$$r\dot{\phi} = v \cos \psi; \quad \dot{r} = v \sin \psi, \quad (5)$$

so that

$$v^2 = \dot{r}^2 + r^2\dot{\phi}^2.$$

Differentiating this relationship and using equations (2), (3), and (5), we obtain

$$\begin{aligned} v\dot{v} &= \dot{r}\ddot{r} + r^2\dot{\phi}\ddot{\phi} + r\dot{\phi}^2\dot{r} \\ &= \dot{r} \{ r\dot{\phi}^2 - K/r^2 + (L/M) \cos \psi - (D/M) \sin \psi + (T/M) \sin (\psi + \alpha + \beta) \} \\ &+ r\dot{\phi} \{ -2\dot{r}\dot{\phi} - (L/M) \sin \psi - (D/M) \cos \psi + (T/M) \cos (\psi + \alpha + \beta) \} + r\dot{\phi}^2\dot{r} \\ &= v \sin \psi \{ -K/r^2 + (L/M) \cos \psi - (D/M) \sin \psi + (T/M) \sin (\psi + \alpha + \beta) \} \\ &+ v \cos \psi \{ - (L/M) \sin \psi - (D/M) \cos \psi + (T/M) \cos (\psi + \alpha + \beta) \}. \end{aligned}$$

Combining terms, we have

$$\dot{v} = - (K/r^2) \sin \psi - (D/M) + (T/M) \cos (\alpha + \beta). \quad (6)$$

This can also be written as

$$\dot{v} = (T/M) \cos \beta \cos \alpha - (D/M) - (K/r^2) \sin \psi - (T/M) \sin \beta \sin \alpha, \quad (6')$$

and this is the form of Ehrlicke's Eq. (5-23) [2]. To obtain the equation for  $\psi$ , we differentiate Eq. (5):

$$\dot{v} \cos \psi - v (\sin \psi)\dot{\psi} = \dot{r}\dot{\phi} + r\ddot{\phi}.$$

Hence,

$$v (\sin \psi)\dot{\psi} = \left[ -\frac{K}{r^2} \sin \psi - \frac{D}{M} + \frac{T}{M} \cos (\alpha + \beta) \right] \cos \psi - \dot{r}\dot{\phi}$$

$$+ 2\dot{r}\dot{\phi} + \frac{L}{M} \sin \psi + \frac{D}{M} \cos \psi - \frac{T}{M} \cos (\psi + \alpha + \beta).$$

Combining terms and using Eq. (5), we have

$$v\dot{\psi} = - \left[ \frac{K}{r^2} - \frac{v^2}{r} \right] \cos \psi + \frac{T}{M} \sin (\alpha + \beta) + \frac{L}{M}. \quad (7)$$

This can be written as

$$v\dot{\psi} = \frac{T}{M} \cos \beta \sin \alpha + \frac{L}{M} + \frac{T}{M} \sin \beta \cos \alpha - \left[ \frac{K}{r^2} - \frac{v^2}{r} \right] \cos \psi, \quad (7')$$

which corresponds to the form of Ehricke's Eq. (5-27) [2]. The derivation of Eqs. (6) and (7) is very similar to Ruppe's procedure for obtaining his Eqs. (3.3) and (3.4) [3].

The first level of simplification, which is analyzed elsewhere [2,3], results from the fact that for the large launch vehicles of interest here,  $\beta \ll \alpha$ , so that the equations of motion simplify to

$$\dot{v} \simeq - (K/r^2) \sin \psi - (D/M) + (T/M) \cos \alpha \text{ and} \quad (8)$$

$$v\dot{\psi} \simeq - \left[ (K/r^2) - (v^2/r) \right] \cos \psi + (L/M) + (T/M) \sin \alpha. \quad (9)$$

Another great simplification results when one finds [2,3] that the increase of thrust at higher altitudes is approximately cancelled by the drag effect in the calculation of cutoff conditions. Small  $\alpha$  is normally a requirement when aerodynamic forces are a factor (e.g., for first-stage motion or altitudes less than 60 km). Under these conditions the lift can be written as in Ref. 2:

$$L \simeq C_L S \rho v^2/2 \simeq (\partial C_L/\partial \alpha) \alpha S \rho v^2/2, \quad (10)$$

where  $S$  is a reference cross-sectional area of the vehicle,  $\rho$  is the atmospheric density, and  $\partial C_L/\partial \alpha$  is a constant determined from wind-tunnel testing. Hence, at this level of simplification,

$$\dot{v} \simeq - (K/r^2) \sin \psi + (T/M) \cos \alpha \quad (11)$$

and

$$v\dot{\psi} \simeq - \left[ \frac{K}{r^2} - \frac{v^2}{r} \right] \cos \psi + \frac{T}{M} \left\{ 1 + \frac{\partial C_L}{\partial \alpha} \frac{S \rho v^2}{2T} \right\} \sin \alpha, \quad (12)$$

one can do relatively simple calculations. Small  $\alpha$  ascent is desirable from the standpoint of launch efficiency, i.e., minimum fuel expenditure for accomplishing the mission [2,3]. Thrust is considered to be a constant in Eqs. (11) and (12), with

$$T = \dot{M} v_e. \quad (13)$$

Here  $v_e$  is the effective speed with which exhaust gases are ejected relative to the nozzle exit aperture [3], and  $\dot{M}$  is the rate at which exhaust mass is ejected. One simplified, approximate procedure for equations (11) and (12) is to: (a) assume a programmed deflection function  $\psi(t)$  for the various launch vehicle stages, which results in correct orbit entry conditions at burnout, (b) solve Eq. (11) by integration, and (c) compute angle of attack from (12). The last step in this procedure is simply to check the assumption of reasonably small  $\alpha$  used in obtaining Eqs. (11) and (12). In this context  $\alpha$  is given as the solution of

$$\sin \alpha = \frac{Mv\dot{\psi} + M (K/r^2) [1 - vr^2/K] \cos \psi}{T \{1 + (\partial C_L / \partial \alpha) S \rho v^2 / 2T\}} \quad (14)$$

This equation turns out to be identical to the result derived by Ehrlicke (cf. his Eqs. (6-40), (6-42), and (6-50)), *except* for the square-bracketed term in Eq. (14), which Ehrlicke refers to as a centrifugal load factor [2]. He introduces this factor in an ad hoc fashion, and he apparently incorrectly replaces  $v$  in this factor by  $v \cos \theta$ . Ehrlicke shows that for a large winged rocket vehicle the term enclosed in braces in the denominator substantially reduces angle of attack  $\alpha$  beneath its vacuum value, particularly for the first stage of the launch vehicle [2].

Normally,  $\alpha$  is small in first-stage motion when aerodynamic effects are important, but can be fairly large in higher stage motion when aerodynamic forces are insignificant, depending on required orbit injection conditions. The presence of the  $\cos \alpha$  term in Eq. (11) can thus be important for higher stages.

### Integration of the Equations of Motion

We follow Ehrlicke's notation [2] in integrating Eq. (11) for a particular stage of a multi-stage rocket vehicle. We introduce  $t_1$  as the burn duration of the stage and the normalized time variable  $\xi$  for that stage:

$$\xi = t/t_1. \quad (15)$$

Here  $\xi$  varies between 0 and 1. During this time, mass varies as

$$M/M_o = (M_o - \dot{M}t)/M_o = 1 - \frac{\dot{M}t}{M_o} = 1 - \xi\Lambda, \quad (16)$$

where

$$\Lambda \equiv \dot{M}t_1/M_o \equiv W_p/W_o \quad (17)$$

is a parameter which is given as the weight of propellant for that stage divided by the initial weight of the launch vehicle at that stage. If we assume small angles of attack, such that  $\cos \alpha \approx 1$ , and normalize the vehicle speed to the exit speed of the exhaust gases, i.e., define

$$\chi \equiv v/v_e, \quad (18)$$

we find easily (cf. Eq. (6-24) in Ref. [2]) that

$$\Delta v/v_e = \Delta\chi \equiv \chi - \chi_o = -\ln(1 - \xi\Lambda) - (\Lambda/n_o) (I_\theta)_\xi, \quad (19)$$

where  $n_o$  is the thrust-to-weight ratio

$$n_o = T/M_o g(R) = T/W_o, \quad (20)$$

where  $g(r) = K/r^2$  is the acceleration of gravity, and

$$(I_\theta)_\xi \equiv \int_0^\xi \frac{g(r)}{g(R)} \sin \psi d\xi'. \quad (21)$$

Here  $\psi$  varies from its value at the beginning of the particular stage, which is the same as its cutoff value at the end of the preceding stage (intermediate coasting can be included as a separate stage), to its value at the particular time according to a well-defined prescription for  $\psi(\xi)$ . Ehrlicke uses a deflection program such that  $\psi$  vanishes at  $\xi = 0$  and 1 and  $\dot{\psi} = 0$  at  $\xi = 1$  [2]. This is not necessarily optimum. The integration in Eq. (21) is performed by a simple numerical method, and so  $\chi(\xi)$  in Eq. (19) is determined at the particular  $\xi$  mesh points selected for the numerical integration. Ruppe [3] gives a procedure for obtaining analytic results. Then from Fig. 1 and Eq. (5), altitude and ground range are determined from

$$\begin{aligned} y - y_o &= v_e t_1 \int_0^\xi \chi \sin \psi d\xi \\ x - x_o &= v_e t_1 \int_0^\xi \chi \cos \psi \frac{R}{R + y} d\xi = R(\phi - \phi_o). \end{aligned} \quad (22)$$

From Eq. (14), the angle of attack is found from

$$\sin \alpha = \frac{\left(\frac{R}{r}\right)^2 \left[1 - \frac{v^2 r}{K}\right] \left[\frac{1 - \xi \Lambda}{n_o} \cos \psi\right] + \frac{\chi}{\Lambda} (1 - \xi \Lambda) \frac{d\psi}{d\xi}}{\left\{1 + \frac{\partial C_L}{\partial \alpha} \frac{S \rho v^2}{2T}\right\}}. \quad (23)$$

The initial parameters  $\chi_o$ ,  $x_o$ , and  $y_o$  for the particular stage in question are the same as the cutoff values for the preceding stage. For the very first stage  $x_o = y_o = 0$ , and we would use  $\chi_o = 0$  in our calculations. We should reiterate, however, that earth's rotation effects have not been included. Fortunately, the additional complications caused by their inclusion do not present unsurmountable problems, as we will attempt to demonstrate in the next section.

### 3. INCLUSION OF EARTH'S ROTATION

The preceding equations would be valid in an inertial frame of reference if all effects of a rotating earth could be excluded. One effect of a rotating earth is to impart an initial velocity to the rocket at launch. If this were the only effect, this velocity could be simply vectorially added to the velocities found in the preceding section and integrated to give a correction to altitude and ground coordinates. There is another effect, however; the earth's atmosphere corotates with the earth to a first approximation (disregarding the ordinary winds experienced by an earth observer). If the atmosphere were stationary in an inertial reference frame, an earth observer would be subjected to constant wind speed of  $903 \cos L$  knots, where  $L$  is the terrestrial latitude of the observer. This suggests that an exact solution of the rocket problem might profitably be carried out in a frame of reference which rotates with the earth, at least while aerodynamic effects are important. This is the basis of an approximation suggested by Ruppe [3]. For the sake of this discussion, we suppose that the first stage of our multistage rocket vehicle corresponds to the period of rocket flight when aerodynamic effects are important. Ruppe suggests [3] that the equations of motion should be solved in the rotating reference frame (in which the atmosphere is stationary) for the first stage, that the results should be transformed back to the inertial frame of reference, and subsequent stages treated in the inertial frame, since aerodynamic effects are unimportant for the higher stages. The transformation from the rotating reference frame back to the inertial reference frame after cutoff of the first stage gives

$$\Delta \mathbf{v}_1 = \Delta \mathbf{v}_{R1} + \mathbf{v}_o, \quad (24)$$

where  $\Delta \mathbf{v}_1$  is the rocket velocity in the inertial frame after cutoff of stage 1, and  $\Delta \mathbf{v}_{R1}$  is the same velocity determined in the rotating reference frame. From the general theory of such transformations (see, e.g., Ref. 5)

$$\mathbf{v}_o = \underline{\omega}_E \times \mathbf{r}_1 \simeq \omega_E R \left( 1 + \frac{y_1}{R} \right) \cos L_o \hat{E} \equiv \mathbf{v}_o \hat{E}, \quad (25)$$

where  $\mathbf{r}_1$  is the radius vector to the satellite, and  $y_1$  its altitude after cutoff of the first stage. The approximation indicated in Eq. (25) is associated with a "flat earth" approximation for the first-stage motion in which the curvature of the earth is disregarded, so that  $L_o$  is the latitude of the launch point, and  $\hat{E}$  is a unit vector in the easterly direction at the time and place of launch. This approximation, which is discussed later, is very often valid for first-stage motion, and for the modest altitudes attained, one sees that  $\mathbf{v}_o$  is approximately the velocity imparted to the rocket at its launch point by earth's rotation in an inertial frame. The magnitude of  $\omega_E R$  is [5] 465 m/s (1524 ft/s) = 903 knots. The true inertial velocity during the  $k$ th stage is given by

$$\mathbf{v}(t_1 + t_2 + \dots + \xi t_k) = \mathbf{v}_o + \Delta \mathbf{v}_{R1} + \Delta \mathbf{v}_2 + \dots + (\Delta \mathbf{v}_k)_\xi \equiv \mathbf{v}_o + \mathbf{v}'. \quad (26)$$

Here  $\Delta \mathbf{v}_j (j > 1)$  is the velocity increment of the  $j$ th stage (computed as in the previous section), and  $(\Delta \mathbf{v}_k)_\xi$  is the velocity increment in the  $k$ th stage. The entity  $t_j$  is the burn duration time for the  $j$ th stage, and  $\xi$  is the reduced time variable which varies between 0 and 1 (cf. Eq. (15)). We shall find  $\Delta \mathbf{v}_{R1}$  later and justify that it and  $\mathbf{v}'$  in Eq. (34) are approximately coplanar, just as in the previous section. But for now, we simply assume this fact and proceed to carry out the vector addition of  $\mathbf{v}_o$  and  $\mathbf{v}'$  in Eq. (26). We do this with the help of Fig. 3, which shows the planar motion represented by  $\mathbf{v}'$  and the vector  $\mathbf{v}_o$  drawn from the launch point in an easterly direction. The orientation of the plane of  $\mathbf{v}'$  is specified by the azimuth angle  $a_o$  measured from north (N) to east (E) at the launch point. The vector  $\mathbf{v}'$  is specified by its magnitude  $v'$  and by its direction, which can be determined from  $a_o$ , the heading  $\psi'$ , and the ground range angle  $\phi'$ , all of which are indicated in Fig. 3. To facilitate the vector addition, we break  $\mathbf{v}_o$  into a component  $\mathbf{v}_{o\perp}$  perpendicular to the plane of  $\mathbf{v}'$  and a component  $\mathbf{v}_{o\parallel}$  in this plane. Evidently,

$$\mathbf{v}_{o\perp} = \mathbf{v}_o \cos a_o \quad \text{and} \quad \mathbf{v}_{o\parallel} = \mathbf{v}_o \sin a_o. \quad (27)$$

Hence,  $\mathbf{v}$  can be specified as the sum of three perpendicular component vectors (shown in Fig. 4),

$$\mathbf{v} = \mathbf{v}_v + \mathbf{v}_h + \mathbf{v}_{o\perp}, \quad (28)$$

where  $\mathbf{v}_v$  is parallel to the radius vector from the center of the earth to the rocket, and  $\mathbf{v}_h$  is perpendicular to it, but in the plane of  $\mathbf{v}'$ . From the geometry in Fig. 4 it follows that

$$\begin{aligned} \mathbf{v}_h &= v' \cos \psi' + \mathbf{v}_{o\parallel} \cos \phi', \\ \mathbf{v}_v &= v' \sin \psi' + \mathbf{v}_{o\parallel} \sin \phi', \end{aligned} \quad (29)$$

and

$$v = [v_v^2 + v_h^2 + v_{o\perp}^2]^{1/2}.$$

The true heading  $\psi$  with respect to the local horizontal is given by

$$\sin \psi = v_v / v. \quad (30)$$



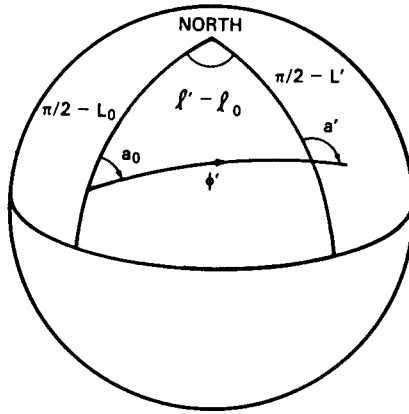


Fig. 5 — Flight path projection of two-dimensional rocket motion on a nonrotating earth

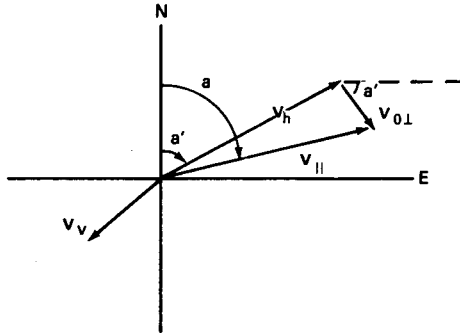


Fig. 6 — Vector diagram for azimuth angle determination taking into account earth's rotation

We thus have completed the vector addition of Eq. (26). With the knowledge of  $v$ ,  $\psi$ , and  $a$ , we can determine the actual position of the space vehicle in an inertial coordinate system. We can describe these position coordinates as the altitude of the space vehicle plus the latitude and longitude of its flight projection on the surface of the earth in an inertial geocentric-equatorial coordinate system [5]. (In this system the latitude-longitude grid is fixed in space.) With

$$\chi \equiv v/v_e, \quad (33)$$

we have

$$y - y_0 = v_e t_1 \int_0^\xi \chi \sin \psi d\xi'$$

$$L - L_0 = v_e t_1 \int_0^\xi \frac{\chi \cos \psi}{R + y} \cos a d\xi'$$

$$l - l_0 = v_e t_1 \int_0^\xi \frac{\chi \cos \psi}{R + y} \sin a \, d\xi' \quad (34)$$

for the *changes* in altitude, latitude, and longitude during a particular burn stage of the rocket vehicle. The parameters in the above integrals are evaluated for values of  $\xi'$  between 0 and  $\xi$ , where  $\xi = 0$  is associated with cutoff of the preceding stage, and  $\xi = 1$  is associated with cutoff of the present stage.

The preceding expressions, particularly those which invoke the approximation in Eq. (25), can be considered valid in a flat earth approximation for the first stage—the period of rocket ascent when aerodynamic effects are significant. This approximation for any part of rocket motion can be considered valid, for example, when  $\phi'$  can be disregarded, as in Eqs. (29) and (31). We note, for example, that a ground range of 500 n.mi. corresponds to  $\phi' \simeq 8.3^\circ$ . For this value  $\sin \phi'$  is only about 1/7 the value of  $\cos \phi' = 0.99$ , so that  $\sin \phi' = 0$  and  $\cos \phi' = 1$  is an adequate approximation, particularly for the significant portion of rocket trajectory when  $v' \gg v_0$ . Hence, as long as the first-stage motion covers a ground range of 500 n.mi. or less, or  $\phi' < 10^\circ$ , we have a sufficient condition for the validity of the flat earth approximation for the first stage. This condition is very often satisfied by first-stage motion, although in our equations it does not have to be satisfied by higher stages of a multistage rocket.

It is possible to go beyond the flat earth approximation for the first stage, and we already have done so in the statement of Eq. (25). The initial problem of using  $\mathbf{v}_0 = \underline{\omega}_E \times \mathbf{r}_1$  is that we don't know  $\mathbf{r}_1$  ahead of time, since it is determined as a subsequent step based on the velocity determination. We have exploited a flat earth approximation to substitute for  $\mathbf{r}_1$  a vector from the center of the earth through the launch point. This allowed us to determine  $\mathbf{v} = \mathbf{v}_0 + \mathbf{v}'$ , where  $\mathbf{v}'$  was computed without the effects of a rotating earth. This itself is only an approximation for the contribution  $\Delta \mathbf{v}_{R1}$  to  $\mathbf{v}'$ , although we shall see later that it is quite a good one. With  $\mathbf{v}(t)$  determined,  $\mathbf{r}(t)$  followed from Eqs. (27) through (34). Next, one may choose to investigate the earth's curvature effect for the first stage by substituting  $\mathbf{r}_1$  from this determination into  $\mathbf{v}_0 = \underline{\omega}_E \times \mathbf{r}_1$  as the start of another iteration. The vector  $\mathbf{r}_1$  will be specified by the inertial coordinates  $y_1$ ,  $L_1$ , and  $l_1$ . From then on, the computations of Eqs. (26) through (34) are repeated, with some modifications, in this new iteration. The modifications are necessitated by the new orientation of the vector  $\mathbf{v}_0$ . The true flight path, at least the one determined from the calculation which preceded the new iteration, is shown in Fig. 7 along with other data which will be used to determine the aforementioned modifications. Also shown is the flight path for  $\mathbf{v}'$ . The easterly direction at  $(L_1, l_1)$  is the same as that at  $(L'_1, l_1)$ . We will use the given information about the spherical triangle ABC in Fig. 7 (namely, the two angles  $l_1 - l_0$  and  $a_0$  and included side  $\pi/2 - L_0$ ) to determine azimuth angle  $a_1$  and  $\phi'_1$ , which is the angular distance in the plane of  $\mathbf{v}'$  associated with the first stage. These calculations will specify the orientation of  $\mathbf{v}_0$ . From standard spherical trigonometry formulae [1], we have

$$\cot\left(\frac{\pi}{2} - L'_1\right) \sin\left(\frac{\pi}{2} - L_0\right) = \cos\left(\frac{\pi}{2} - L_0\right) \cos(l_1 - l_0) + \sin(l_1 - l_0) \cot a_0$$

or

$$\tan L'_1 = (\cos L_0)^{-1} \left[ \sin L_0 \cos(l_1 - l_0) + \cot a_0 \sin(l_1 - l_0) \right], \quad (35)$$

which determines  $L'_1$ ; then

$$\sin \phi'_1 = \sin(l_1 - l_0) \cos L'_1 / \sin a_0 \quad (36)$$

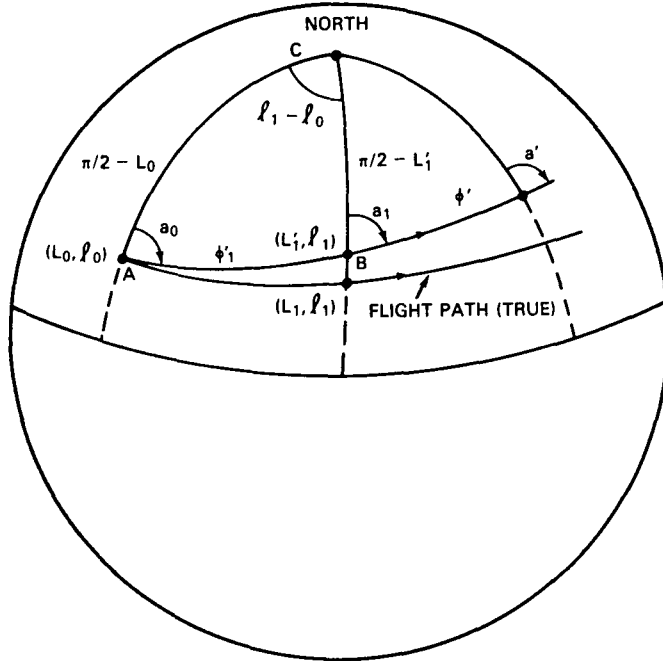


Fig. 7 — Flight path projection on nonrotation latitude-longitude grid. The diagram makes possible the inclusion of earth's rotation and earth's curvature for the first stage.

determines  $\phi'_1$ . Azimuth angle  $a_1$  is found from Eq. (31):

$$\sin a_1 = \sin a_0 \cos L_0 / \cos L_1. \quad (37)$$

Now the modifications of Eqs. (27) through (34) consist of the following:

$$v_{o\perp} = v_o \cos a_1 \quad \text{and} \quad v_{o\parallel} = v_o \sin a_1 - \quad (38)$$

which replaces Eq. (27) —

$$\begin{aligned} v_h &= v' \cos \psi' + v_{o\parallel} \cos(\phi' - \phi'_1), \\ v_v &= v' \sin \psi' + v_{o\parallel} \sin(\phi' - \phi'_1), \end{aligned}$$

and

$$v = [v_v^2 + v_h^2 + v_{o\perp}^2]^{1/2}, \quad (39)$$

which is used instead of Eq. (29); the other equations are unchanged. The new iteration will result in new velocities and positions, which may be made the basis of another iteration, if it is necessary to satisfy convergence criteria.

It remains now to specify  $\Delta \mathbf{v}_{R1}$  in Eq. (26). It is well known (e.g., see Ref. 5) that transformation from an inertial to the rotating frame of reference is accompanied by the addition of effective Coriolis and centrifugal forces in the equations of motion; i.e. [5],

$$d\mathbf{v}_R/dt = d\mathbf{v}_F/dt - 2\boldsymbol{\omega}_E \times \mathbf{v}_R - \boldsymbol{\omega}_E \times (\boldsymbol{\omega}_E \times \mathbf{r}),$$

where the subscripts  $R$  and  $F$  refer to rotating and inertial frames, respectively. When expressed in rotating frame coordinates, the aerodynamic forces associated with the first term on the right properly depend only on rocket motion. The latter two terms are Coriolis and centrifugal terms. We estimate in Appendix C how large the velocity contributions from the various forces might typically be for a large rocket vehicle at cutoff of the first stage [1-3]. In order of decreasing values, we find  $\Delta v_T: \Delta v_G: v_o: \Delta v_D: \Delta v_{Cor}: \Delta v_{cent} = 1000: 300: 150: 50: 10: 1.5$ , where we list, in order, effects of thrust, gravity, initial velocity from earth's rotation, drag (which is approximately cancelled by thrust increase due to ambient pressure decrease [2,3]), Coriolis force, and centrifugal force. These estimates indicate the conclusion that the principal effect of a rotating earth is to add in the velocity  $v_o$  as prescribed in Eqs. (25) and (26) and discussed subsequent to these equations. The Coriolis and centrifugal contributions appear to be very small, so that  $\Delta \mathbf{v}_{R1}$  could be approximated quite well by the approach of Section 2, which disregards the effects of a rotating earth and atmosphere.

The preceding results notwithstanding, one may wish to improve the specification of  $\Delta \mathbf{v}_{R1}$ , particularly if computational simplicity can be preserved. The accuracy can be improved if we include only the component of velocity effect from Coriolis and centrifugal forces in the particular plane of motion which is associated with the disregard of rotational effects. To illustrate the mathematical point that this is a good approximation for the small correction from Coriolis and centrifugal terms, let us consider what happens in Eqs. (29) and (30) when  $\phi' \simeq 0$  and  $v_o \ll v'$ . In Eq. (29) we have

$$v = [v'^2 + 2v'v_{o\parallel} \cos \psi' + v_{o\perp}^2]^{1/2} \simeq v' \left[ 1 + \frac{v_{o\parallel}}{v'} \cos \psi' + 0 \left[ \frac{v_o}{v'} \right]^2 \right],$$

and in Eq. (29)  $\sin \psi \simeq v' \sin \psi' / v$ . In these equations only the component  $v_{o\parallel}$  enters in first order for  $v$  and  $\psi$ . The only first order correction involving  $v_{o\perp}$  that can be found is in the determination of  $a$  in Eq. (32), and this is not important. Hence, along with Ruppe [3], we transform to the rotating frame coordinates in Eqs. (2) and (3) by setting

$$\dot{\phi} = \dot{\phi}_R + \dot{\phi}_o,$$

where

$$\dot{\phi}_o = \boldsymbol{\omega}_E \cos L_o \sin a_o.$$

When Eq. (40) is substituted into Eqs. (2) and (3), and the steps which led to Eqs. (6) and (7) are redone, it is found that

$$\dot{v}_R = - \left[ \frac{K}{r^2} - r\dot{\phi}_o^2 \right] \sin \psi - \frac{D}{M} + \frac{T}{M} \cos(\alpha + \beta) \quad (41)$$

$$v_R \dot{\psi} = - \left[ \frac{K}{R^2} - r\dot{\phi}_o^2 - \frac{v_R^2}{r} \right] \cos \psi + \frac{T}{M} \sin(\alpha + \beta) + \frac{L}{M} + 2v_R \dot{\phi}_o, \quad (42)$$

where

$$\mathbf{v}_R \equiv (\Delta \mathbf{v}_{R1})_{\xi}.$$

The symbol  $(\Delta \mathbf{v}_{R1})_\xi$  has been defined in connection with Eq. (26). One now sees additional Coriolis and centrifugal terms in the equation of motion. In the same way that Eqs. (11) and (12) were obtained, one finds

$$\dot{v}_R \simeq - \left[ \frac{K}{R^2} - r \dot{\phi}_0^2 \right] \sin \psi + \frac{T}{M} \cos \alpha \quad (43)$$

$$v_R \dot{\psi} \simeq - \left[ \frac{K}{r^2} - r \dot{\phi}_0^2 - \frac{v_R^2}{r} \right] \cos \psi + \frac{T}{M} \left\{ 1 + \frac{\partial C_L}{\partial \alpha} \frac{S \rho v_R^2}{2T} \right\} \sin \alpha + 2v_R \dot{\phi}_0. \quad (44)$$

In terms of a programmed deflection function  $\psi(t)$ , one obtains the angle of attack  $\alpha$  from

$$\sin \alpha = \frac{M v_R (\dot{\psi} - 2\dot{\phi}_0) + M(K/r^2) [1 - v_R^2 r/K - r^3 \dot{\phi}_0^2/K] \cos \psi}{T \{1 + (\partial C_L/\partial \alpha) S \rho v_R^2/2T\}}. \quad (45)$$

The solution for  $v_R$  is found as in Eq. (19). It is

$$\chi' \equiv v_R/v_e = \chi'_0 1 - \ln(1 - \xi \Lambda) - (\Lambda/n'_0) (I_\theta)_\xi, \quad (46)$$

where  $\xi$  and  $\Lambda$  are given by Eqs. (15) and (17), respectively, and

$$n'_0 = T/M_0 g'(R) = T/W'_0. \quad (47)$$

Here,

$$g'(r) = K/r^2 - r \dot{\phi}_0^2 = g(r) - r \dot{\phi}_0^2 \quad (48)$$

is an "apparent" acceleration of gravity and

$$(I_\theta)_\xi = \int_0^\xi \frac{g'(r)}{g'(R)} \sin \psi \, d\xi'. \quad (49)$$

As indicated previously, the centrifugal correction to gravity is only a few tenths of a percent. For the first stage  $\chi'_0 = 0$  and, from Eq. (39), we should include the initial condition

$$\dot{\psi}(0) = 2\dot{\phi}_0 \quad (\text{first stage}) \quad (50)$$

in our programmed deflection function. This is similar to the conclusion reached by Ruppe [3]. Since  $\omega_E = 7.292 \times 10^{-5}$  rad/s, it is seen that  $\dot{\psi}(0)$  in Eq. (50) is of the order of  $5 \times 10^{-3}$  deg/s, which corresponds to  $1^\circ$  in 200 s. Similarly,  $R \dot{\phi}_0^2$  is on the order of  $10^{-2}$  m/s<sup>2</sup>. These are evidently very small corrections, in accordance with our previous estimates, so that  $\Delta \mathbf{v}_{R1}$  in Eq. (24) and  $\mathbf{v}'$  in Eq. (26) could be computed to a good first approximation as if there were no earth's rotation effects.

The computational procedure for relatively simple analyses of powered rocket ascent is now clear; it may be summarized as follows. The most significant part of the rocket trajectory is assumed to be above the atmosphere and associated with second and higher stages, with  $v_0 \ll v'$ , so that for any qualitative analysis one may ignore earth's rotation effects. For this purpose, one uses: (a) a programmed deflection function  $\psi(r)$  [2,3]; (b) a thrust given by Eq. (13) with correctly chosen exhaust velocity  $v_e$  [3,6], (c) Eqs. (15) through (22) for the velocity, altitude, and ground range of the rocket in all stages, where  $r = R$  is an expedient approximation for low altitude rocket flights and analytic results [3]; (d) Eq. (23) for checks on the smallness of the angle of attack; and (e) Eq. (31) for the determination of earth's curvature

effects in the computation of latitude, azimuth angle, and longitude of the rocket flight path projection on the surface of a nonrotating earth (hence, an inertial latitude-longitude grid). If the conditions warrant a flat earth approximation, as determined by the ground range calculation (e.g., if  $\phi' \leq 10^\circ$ ), then step (e) can be dispensed with. Also, if the approximation  $r \approx R$  has been made in step (c), one may improve these results by starting with them in another iteration of step (c) without the approximation.

If one wishes to improve quantitative accuracy by taking earth's rotation effects into account, he should find the following summary useful. One could start with the results in the preceding paragraph and simply add in  $v_0$  to the previous velocities  $v$  as in Eq's. (25) and (26), where  $r_1$  was determined in the previous results. Actually, to be consistent, one should redetermine the first-stage results of the preceding paragraph with the use of Eqs. (45) through (50). There probably will be no appreciable differences from the previous first-stage results obtained without regard for earth's rotation effects, but the results should at least be checked. If a flat earth approximation is valid for the first stage, one computes component and total speeds from Eqs. (27) and (29) with the approximation in Eq. (25), heading  $\psi$  from Eq. (30), and azimuth angle  $a$  from Eq. (32). The primed entities in these equations are known at this point, having already been computed. The altitude and flight path projection are computed, presumably through numerical integration, in Eq. (34). If a flat earth approximation is not valid for the first stage, one computes component and total speeds from Eqs. (38) and (39), where  $a'_1$  is substituted for  $a_1$  (primed entities are known). Heading, azimuth angle, altitude, and flight path projection are again determined from Eqs. (30), (32), and (34). These results can then be used as the start of another iteration for obtaining greater accuracy in the inclusion of earth's rotation effects when the flat earth approximation for the first stage is not sufficiently accurate. The description of this iteration procedure is included in the paragraph which includes Eqs. (35) through (39). It is expected that no more than one iteration would be required. Even one iteration might not be worthwhile in view of the basic approximations we have made regarding thrust and aerodynamic effects. The computations are greatly simplified if a flat earth approximation can be made for the total powered rocket trajectory. All that would be required for a complete specification of orbit injection conditions (described in the next section) is the altitude calculation from the preceding paragraph, with possible alterations which might arise from Eqs. (46) through (50) for the first stage and simple vector addition of velocities, as in Eqs. (25) and (26). One could start the other way around, however, with desired orbit injection conditions ( $v$ ,  $\psi$ , and  $a$ ) and obtain the launch profile conditions ( $v'$ ,  $\psi'$ ,  $a_0$ ) needed to obtain them; here  $v'$  and  $\psi'$  are rocket burnout parameters. This method is explained in Appendix D.

Finally, if one wants complete quantitative accuracy regarding all the effects we have mentioned—or if one has sufficient information about aerodynamic effects and other factors of the system, such as drag and lift coefficients, a model atmosphere, thrust variability, etc., and wants to include these effects in his analysis—he may achieve this in a full numerical solution to the problem. The discussion of Kooy [6] is particularly helpful in this regard. Rocket velocity and coordinates can be straightforwardly obtained by Kooy's procedure [6] in a geocentric equatorial coordinate system by a Runge-Kutta integration method. The conversion of these results to latitude, longitude, azimuth, altitude, and heading variations is simple, and is discussed in the next section. Kooy's method appears to be quite feasible, as well as accurate, with the use of modern computers.

#### 4. ORBIT TRAJECTORY FROM INJECTION CONDITIONS AT ROCKET BURNOUT

At the end of powered rocket ascent (i.e., "burnout") the payload is assumed to enter an elliptical orbit above the earth's atmosphere in the spherical gravitational field of the earth. This satellite motion thus satisfies (in an inertial frame)

$$\ddot{\mathbf{r}} + (K/r^3) \mathbf{r} = 0, \quad (51)$$

where  $K = 1.407645 \times 10^{16} \frac{\text{ft}^3}{\text{sec}^2} \approx 6.275 \times 10^4 \frac{(\text{n.mi.})^3}{\text{sec}^2}$  is the same parameter as used previously (see, e.g., Eq. (2)). The small corrections in the equation of motion due to the oblate earth, aerodynamic drag, etc., can be handled by the techniques of perturbation theory [1], but will not be included in the present report. Dotting Eq. (51) with  $\dot{\mathbf{r}}$  and integrating with respect to time, one obtains an energy constant of the motion

$$E = v^2/2 - K/r. \quad (52)$$

Similarly, vector multiplying Eq. (51) by  $\mathbf{r}$  and integrating with respect to time, one obtains an angular momentum constant of the motion:

$$\mathbf{h} = \mathbf{r} \times \dot{\mathbf{r}}. \quad (53)$$

Hence, the motion is planar. Now if one vector multiplies Eq. (51) by  $\mathbf{h}$  and integrates it with respect to time, one finds [1,5]

$$\dot{\mathbf{r}} \times \mathbf{h} = K \left( \frac{\mathbf{r}}{r} + \mathbf{e} \right), \quad (54)$$

where  $\mathbf{e}$  is a vector integration constant. If we define  $\theta$  as the angle between  $\mathbf{e}$  and  $\mathbf{r}$ , the dot product of this equation with  $\mathbf{r}$  yields the orbit equation [1,3]

$$\frac{1}{r} = \frac{K}{h^2} (1 + e \cos \theta), \quad \text{where } e = \sqrt{1 + \frac{2Eh^2}{K^2}} \quad (55)$$

is the eccentricity of the orbit. Fig. 8a shows the elliptical orbit circumscribed about the earth centered at one of the foci, and Fig. 8b shows an associated vector diagram. Also shown are several parameters used in discussing the ellipse and the motion of the satellite. The parameters  $r_p$ ,  $r_a$ ,  $l$ , and  $a$  are the perigee, apogee, latus rectum, and semimajor axis lengths, respectively; their values can be derived from Eq. (55). The angle  $\theta$  is measured from the perigee vector (in the direction of  $\mathbf{e}$ ), as shown in Fig. 8b, and the velocity and heading of the satellite are shown in a manner consistent with their previous use in this report. From the relation

$$\frac{dr}{dt} = -h \frac{d(1/r)}{d\theta} = v \sin \psi \quad (56)$$

and Eq. (55), one obtains [1]

$$\begin{aligned} e \sin \theta &= (rv^2/K) \sin \psi \cos \psi \\ e \cos \theta &= (rv^2/K) \cos^2 \psi - 1. \end{aligned} \quad (57)$$

These are useful relations for many purposes, but we use them here for an unambiguous determination of the injection angle  $\theta_i$  and eccentricity  $e$  in terms of the injection conditions  $r_i$ ,  $v_i$ , and  $\psi_i$  at burnout. The motion of the satellite in orbit is thus determined from injection conditions, Eq. (55), in which

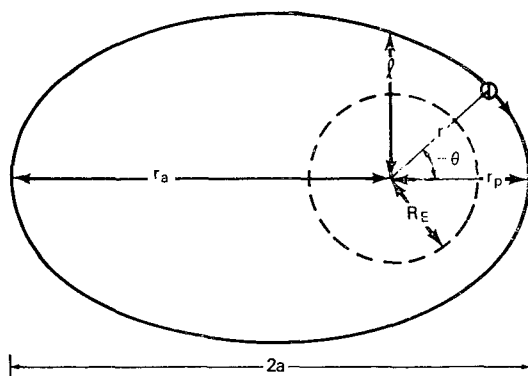


Fig. 8 - (a) The elliptical satellite orbit

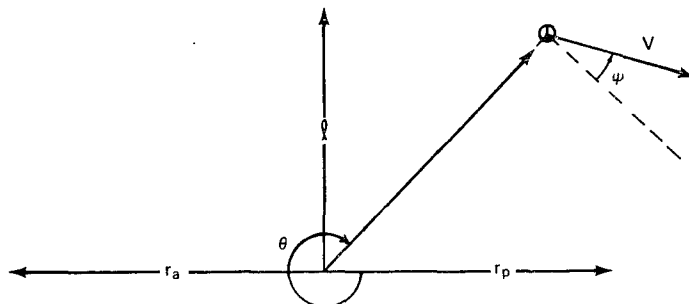


Fig. 8 - (b) Associated vector diagram

$$E = v_i^2/2 - K/r_i \text{ and } h = r_i v_i \cos \psi_i, \quad (58)$$

and the expression for the time  $t_p(\theta)$  it takes a satellite to travel within one revolution from perigee to the angle  $\theta$ . This is [1]

$$t_p(\theta) = \left( \frac{a^3}{K} \right)^{1/2} \left\{ 2 \tan^{-1} \left[ \left( \frac{1-e}{1+e} \right)^{1/2} \tan \frac{\theta}{2} \right] - \frac{e(1-e^2)^{1/2} \sin \theta}{1+e \cos \theta} \right\}. \quad (59)$$

Hence, for example, the time it takes to travel from  $\theta_i$  to  $\theta$  is

$$t(\theta_i \rightarrow \theta) = t_p(\theta) - t_p(\theta_i). \quad (60)$$

The only other thing we need to know is the orientation of the ellipse with respect to the earth in an inertial coordinate system. This can be specified from the vector directions of  $\mathbf{h}$  and  $\mathbf{e}$ , which are determined from injection conditions. Hence

$$\mathbf{h} = \mathbf{r}_i \times \mathbf{v}_i, \quad (61)$$

and from Eq. (52)

$$\mathbf{e} = \frac{1}{K} \mathbf{v}_i \times \mathbf{h} - \frac{\mathbf{r}_i}{r_i} = \frac{1}{K} \left[ \left( v_i^2 - \frac{K}{r_i} \right) \mathbf{r}_i - (\mathbf{r}_i \cdot \mathbf{v}_i) \mathbf{v}_i \right]. \quad (62)$$



$$\begin{aligned}
 \hat{r} &= \cos L \cos \Phi \hat{I} + \cos L \sin \Phi \hat{J} + \sin L \hat{K} \\
 \hat{\Theta} &= \sin L \cos \Phi \hat{I} + \sin L \sin \Phi \hat{J} - \cos L \hat{K} \\
 \hat{\Phi} &= -\sin \Phi \hat{I} + \cos \Phi \hat{J}.
 \end{aligned}
 \tag{66}$$

This completes the orthogonal transformations between the above coordinate systems. Hence, for example, from Eq. (63)

$$\begin{aligned}
 \hat{z} &= [-\sin a \sin L \cos \Phi + \cos a \sin \Phi] \hat{I} \\
 &\quad + [-\sin a \sin L \Phi - \cos a \cos \Phi] \hat{J} \\
 &\quad + \sin a \cos L \hat{K},
 \end{aligned}
 \tag{67}$$

which can be calculated from the orbit injection conditions for  $a$ ,  $L$ , and  $l$ .

Also shown in Fig. 9 are other angles used to describe the orientation of the ellipse in the geocentric equatorial system. These are the inclination  $i$ , the longitude of the ascending node  $\Omega$ , and the argument of perigee  $\beta$ . The inclination angle is the angle between  $\hat{K}$  and  $\mathbf{h}$ , found from Eqs. (63) and (64) to be

$$\cos i = \hat{z} \cdot \hat{K} = -\sin a \hat{\Theta} \cdot \hat{K} = \sin a \cos L.
 \tag{68}$$

In general,  $0 \leq i \leq \pi$  radians, but this equation restricts inclination angles to the range  $|L| \leq i \leq \pi - |L|$ , depending on  $a$ . For inclinations  $0 \leq i < \pi/2$ , we have generally east-erly motion, or so called "direct" orbits [5]. For  $\pi/2 < i \leq \pi$ , we have "retrograde" orbits [5]. If we define the line of nodes as a line from the center of the earth through the point of crossing of the satellite through the equatorial plane, and if the unit vector  $\hat{n}$  has this direction, then

$$\begin{aligned}
 \hat{n} &\equiv (\hat{K} \times \hat{z}) / \sin i \\
 &= \frac{1}{\sin i} [\cos L \cos a \hat{r} + \sin L \cos a \hat{\Theta} - \sin L \sin a \hat{\Phi}].
 \end{aligned}
 \tag{69}$$

This can be evaluated from orbit injection conditions.

Before we can finish the specification of  $\Omega$  and  $\beta$ , we shall need to calculate  $\mathbf{e}$  from Eq. (62):

$$\begin{aligned}
 \mathbf{e} &= \frac{1}{K} \mathbf{v} \times \mathbf{h} - \hat{r} = \left[ \frac{vh}{K} \cos \psi - 1 \right] \hat{r} - \frac{vh}{K} \sin \psi \hat{\Theta} \\
 &= \left[ \frac{vh}{K} \cos \psi - 1 \right] \hat{r} + \frac{vh}{K} \sin \psi [\cos a \hat{\Theta} - \sin a \hat{\Phi}],
 \end{aligned}
 \tag{70}$$

which can be evaluated from orbit injection conditions. For  $\Omega$  one obtains

$$\begin{aligned}
 \cos \Omega &= \hat{n} \cdot \hat{I} = (\sin i)^{-1} \hat{I} \cdot (\hat{K} \times \hat{z}) = -(\sin i)^{-1} \hat{z} \cdot \hat{J} \\
 &= \frac{1}{\sin i} [\sin a \sin L \sin \Phi + \cos a \cos \Phi],
 \end{aligned}
 \tag{71a}$$

where  $0 \leq \Omega \leq 2\pi$  rad in general, but

$$\Omega < \pi \text{ if } \hat{n} \cdot \hat{J} > 0,$$

or its equivalent, if

$$\hat{z} \cdot \hat{I} > 0.$$

Hence, from Eq. (67)

$$\Omega < \pi \text{ if } -\sin a \sin L \cos \Phi + \cos a \sin \Phi > 0. \quad (71b)$$

One also obtains from Eqs. (69) and (70)

$$\begin{aligned} \cos \beta &= e^{-1} \hat{n} \cdot \mathbf{e} \\ &= \frac{1}{e \sin i} \left\{ \cos L \cos a \left[ \frac{vh}{K} \cos \psi - 1 \right] + \sin L \frac{vh}{K} \sin \psi \right\}, \end{aligned} \quad (72a)$$

where  $0 \leq \beta \leq 2\pi$  in general, but if  $\mathbf{e} \cdot \hat{K} > 0$ ,  $\beta < \pi$ , i.e.,

$$\beta < \pi \text{ if } \left[ \frac{vh}{K} \cos \psi - 1 \right] \sin L - \frac{vh}{K} \sin \psi \cos a \cos L > 0. \quad (72b)$$

All the entities in Eqs. (68) through (72) are calculable from known orbit injection conditions, and the specification of the elliptical orbit is complete. For simplicity, one might choose to set  $\Phi_g(0) = 0$  and  $\Phi = l$  in the preceding expressions, which amounts to a redefinition of the  $\hat{I}$  and  $\hat{J}$  directions.

## 5. VEHICLE FLIGHT SEEN BY INERTIAL AND EARTH OBSERVERS

In Sections 2 and 3 the functions for the inertial frame,  $L(t)$ ,  $l(t)$ ,  $y(t)$ ,  $a(t)$ ,  $v(t)$ , and  $\phi(t)$ , were specified for rocket flight. In Section 4 additional information was derived to specify these entities for the orbital flight. We shall specify the first three of these along with the counterpart functions  $L_R(t)$ ,  $l_R(t)$ , and  $y_R(t)$  which describe what the earth observer sees.

It is very simple to deal with the period of powered rocket ascent, i.e., the time frame  $0 \leq t \leq t_i$ , where  $t_i$  is the time after launch to burnout or orbit injection. In Section 3 we have discussed the computation of altitude, latitude, and longitude in an inertial frame, i.e.,  $y(t)$ ,  $L(t)$ , and  $l(t)$ , respectively, during this time period; the solution for  $y_R(t)$  and  $L_R(t)$  is thus also found, since

$$y_R(t) = y(t), \quad L_R(t) = L(t). \quad (73)$$

The function  $l_R(t)$  is simply found from

$$l_R(t) = l(t) - \omega_E t, \quad (74)$$

where

$$\omega_E = 7.292 \times 10^{-5} \text{ rad/s} = 15.04 \text{ deg/h}; \quad (75)$$

see Eq. (35) and [1.5].

For the time frame  $t > t_i$ , the satellite is in the elliptical orbit trajectory discussed in the preceding section. The angle  $\theta$  in Fig. 9 is increasing in the direction of motion of the satellite, by definition, so a computational procedure is to pick a set of increasing  $\theta$  values, starting with

$\theta_i$  determined from Eq. (57) and orbit injection conditions, and to determine an associated set of times from Eqs. (59) and (60), starting with  $t = t_i$ . From spherical trigonometry formulae on the right spherical triangle ABC in Fig. 9, the law of sines determines latitude  $L(t) = L_R(t)$  at these times from

$$\sin L(t) = \sin i \sin [\beta + \theta(t)], \quad (76)$$

where  $\theta(t)$  is given, and  $\beta$  and  $i$  have previously been computed from orbit injection conditions by Eqs. (68) and (72). A cotangent formula [1] determines  $l(t)$  at these times from

$$\tan [l(t) + \Phi_g(0) - \Omega] = \tan [\beta + \theta(t)] \cos i, \quad (77)$$

where  $\Omega$  is determined from injection conditions by Eq. (71), and  $l_R(t)$  is given by Eq. (72). Finally, altitude  $y(t)$  is determined from the known orbit in Eq. (53) by the formula

$$y(t) = y_R(t) = r[\theta(t)] - R(t), \quad (78)$$

where  $R(t)$  is the radius of the earth, which can be taken as approximately constant, and  $r[\theta(t)]$  for the orbit is given by Eq. (55).

## 6. DISCUSSION

In Sections 2 and 3 this report develops the equations required for an analysis of powered rocket trajectory. Most of the effort has been concentrated on the approximations which permit the simpler analysis techniques; the approach to the more complex, completely quantitative numerical methods, however, has at least been indicated. The computational procedures for various levels of simplicity and approximation are delineated by summary discussions near the end of Section 3. The investigator can thus choose the procedure which fits his needs. It was recognized that a radial gravitational field introduces centrifugal terms in an inertial frame, terms which are omitted from some literature sources or given incorrectly. A systematic procedure for taking earth's rotation effects (including atmosphere corotation) into account was also described, a subject often treated incompletely in the literature. Perhaps the most significant contribution of this report is the treatment of earth's curvature effects and how the earth's rotation effects are integrated with it in the simpler analyses of powered rocket trajectory. The literature treatments of approximate analyses of powered rocket trajectory, at least those seen by the author, stay within the confines of the flat-earth approximation; this approximation is discussed in Section 3. The full numerical solution of the rocket problem [6] does typically include earth's curvature effects.

One of the major approximations of simpler analysis techniques of powered rocket trajectory is the cancellation of drag and thrust increase effects. This approximation appears to be quite good for many rockets [2,3], i.e., within 2% for strategic choice of the constant thrust value for each stage [3]. For large rockets, however, the thrust increase effect is expected to more than counterbalance the drag effect, so that one may wish to include these effects explicitly for greater quantitative accuracy. The simplification from constant thrust is then lost from the analysis, but it is eliminated anyway when angles of attack become large, as they frequently do in higher stage motion. One may then wish to solve equations (8) and (9) in Section 2, or equations (10) and (11), by numerical integration (e.g., by the Runge-Kutta method). Information about thrust increase and aerodynamic effects is included in Appendix E. For somewhat greater understanding and control of the launch trajectory, one may wish to assume a profile  $\alpha(t)$  for the angle of attack and solve for the flight path heading  $\psi$  and for speed in the course of the numerical interaction, a job suited for a computer. Previously, we had suggested, for simplicity, an assumed  $\psi(t)$  profile in the calculations.

Section 4 relates the rocket burnout parameters obtained in Sections 2 and 3 to the specification of the elliptical orbit subsequently traversed by the payload and to the point on this orbit where it is injected. The equations are developed somewhat more clearly and completely than usual here, and it is hoped that the orbit determination part of the trajectory analysis is thus facilitated.

In Section 5 the trajectory coordinates of the powered rocket ascent and orbital flight are determined as the altitude and the latitude and longitude of the flight projection on the earth's surface as a function of time after launch. Two cases are considered: (1) the trajectory as seen by a heavenly, inertial observer on a space-fixed latitude-longitude grid on the earth, and (2) the more important case of the common earth-fixed observer who rotates underneath the orbit and sees the rocket and payload from a different perspective. Actually, the first case is just obtained as an intermediate step to the determination of the second case.

There are other perturbations which have not been considered in this report, such as the effect of the oblate earth, variations in aerodynamic forces, solar radiation pressure, etc. [1] Some of these effects alter the long term orbital motion of satellites, which is of no particular consequence for many simple analyses or for this report, which concerns itself with powered rocket ascent and short-term orbit motion. Variable winds on the rocket are assumed to be corrected for in flight as part of the vehicle steering control.

## 7. ACKNOWLEDGMENTS

The author appreciates helpful comments from Dr. John N. Hayes on the manuscript, as well as discussions with Dr. Henry N. Ho.

## 8. REFERENCES

1. K. J. Ball and G. F. Osborne, *Space Vehicle Dynamics*, Oxford University Press, New York, 1967.
2. K. A. Ehricke, *Space Flight II. Dynamics*, D. Van Nostrand Co., New York, 1962.
3. H. O. Ruppe, *Introduction to Astronautics, Vol. 1*, Academic Press, New York, 1966.
4. See, e.g., G. Joos, *Theoretical Physics, 3rd ed.*, Hafner Publishing Co., New York, p. 120.
5. R. R. Bate, D. D. Mueller, and J. E. White, *Fundamentals of Astrodynamics*, Dover Publications, New York, 1971.
6. J. M. J. Kooy, "Dynamics of Controlled Rocket Launching," pp. 31-69 in *Dynamics of Rockets and Satellites*, ed. by G. V. Groves, North-Holland Pub. Co., Amsterdam, 1965.

## Appendix A

### LAGRANGIAN METHOD, INCLUDING THE PRESENCE OF NONCONSERVATIVE FORCES

A system of particles is effectively in equilibrium under the influence of all applied and inertial forces. The applied forces may be further classified as conservative (derivable as the negative gradient of a scalar potential) or nonconservative. We may define the forces as follows:

$$\begin{aligned} \mathbf{F}_i &= -\frac{\partial U_i}{\partial \mathbf{x}_i}: && \text{Conservative force on } i\text{'th particle} \\ \mathbf{F}'_i &: && \text{Nonconservative force on } i\text{'th particle} \\ -m_i \ddot{\mathbf{x}}_i &: && \text{Inertial force on } i\text{'th particle.} \end{aligned} \quad (\text{A1})$$

Newton's equation of motion is

$$\mathbf{F}_i + \mathbf{F}'_i - m_i \ddot{\mathbf{x}}_i = 0, \quad (\text{A2})$$

here restated as particle equilibrium under all three kinds of forces. Since each particle is in effective equilibrium, an arbitrary, infinitesimal, virtual displacement of all the particles will involve no work. This is known as d'Alembert's principle of virtual displacements. Hence

$$\sum_i (\mathbf{F}_i + \mathbf{F}'_i - m_i \ddot{\mathbf{x}}_i) \cdot \delta \mathbf{x}_i = 0. \quad (\text{A3})$$

Because of constraints in the problem (e.g., boundaries, rigid body constraints of the particles, etc.), particle motion will depend on a smaller set of coordinates (e.g., angles of rotation, the center of mass coordinates, etc.), which are referred to [4] as independent generalized coordinates  $q_1, \dots, q_f$ . Hence,

$$\mathbf{x}_i = \mathbf{x}_i(q_1, q_2, \dots, q_f), \quad (\text{A4})$$

$$\delta \mathbf{x}_i = \sum_j [\partial \mathbf{x}_i / \partial q_j] \delta q_j. \quad (\text{A5})$$

Therefore,

$$\dot{\mathbf{x}}_i = \dot{\mathbf{x}}_i(q_1, \dots, q_f; \dot{q}_1, \dots, \dot{q}_f). \quad (\text{A6})$$

One obtains

$$\begin{aligned} \sum_i m_i \ddot{\mathbf{x}}_i \cdot \delta \mathbf{x}_i &= \sum_i \sum_j m_i \ddot{\mathbf{x}}_i \cdot \frac{\partial \mathbf{x}_i}{\partial q_j} \delta q_j \\ &= \sum_i \sum_j m_i \left\{ \frac{d}{dt} \left[ \dot{\mathbf{x}}_i \cdot \frac{\partial \mathbf{x}_i}{\partial q_j} \right] - \dot{\mathbf{x}}_i \cdot \frac{d}{dt} \frac{\partial \mathbf{x}_i}{\partial q_j} \right\} \delta q_j \\ &= \sum_i \sum_j m_i \left\{ \frac{d}{dt} \left[ \dot{\mathbf{x}}_i \cdot \frac{\partial \dot{\mathbf{x}}_i}{\partial \dot{q}_j} \right] - \dot{\mathbf{x}}_i \cdot \sum_k \frac{\partial^2 \mathbf{x}_i}{\partial q_j \partial q_k} \dot{q}_k \right\} \delta q_j \end{aligned}$$

$$\begin{aligned}
 &= \sum_j \left\{ \frac{d}{dt} \left( \frac{\partial}{\partial \dot{q}_j} \sum_i \frac{1}{2} m_i \dot{x}_i^2 \right) - \sum_i m_i \dot{x}_i \cdot \frac{\partial}{\partial q_j} \left( \sum_k \frac{\partial \mathbf{x}_i}{\partial q_k} \dot{q}_k \right) \right\} \delta q_j \\
 &= \sum_j \left[ \frac{d}{dt} \frac{\partial}{\partial \dot{q}_j} \sum_i \frac{1}{2} m_i \dot{x}_i^2 - \frac{\partial}{\partial q_j} \sum_i \frac{1}{2} m_i \dot{x}_i^2 \right] \delta q_j.
 \end{aligned}$$

It is also true that

$$\sum_i \mathbf{F}_i \cdot \delta \mathbf{x}_i = \sum_i - \frac{\partial U_i}{\partial \mathbf{x}_i} \cdot \delta \mathbf{x}_i = \sum_i - dU_i = - \sum_j \frac{\partial}{\partial q_j} \left( \sum_i U_i \right) \delta q_j$$

and

$$\sum_i \mathbf{F}'_i \cdot \delta \mathbf{x}_i = \sum_i \sum_j \mathbf{F}'_i \cdot \frac{\partial \mathbf{x}_i}{\partial q_j} \delta q_j.$$

Hence, if we include the kinetic energies and conservative forces in the Lagrangian  $L$  as

$$L(\dots, q_j, \dot{q}_j, \dots) = \sum_i \left[ \frac{1}{2} m_i \dot{x}_i^2 - U_i(\dots, q_j, \dots) \right], \quad (\text{A7})$$

where  $\dot{x}_i$  is determined by differentiating Eq. (A4), then Eq. (A3) can be written as

$$\sum_j \left[ \frac{d}{dt} \frac{\partial L}{\partial \dot{q}_j} - \frac{\partial L}{\partial q_j} - F_{q_j} \right] \delta q_j = 0, \quad (\text{A8})$$

where

$$F_{q_j} = \sum_i \mathbf{F}'_i \cdot \frac{\partial \mathbf{x}_i}{\partial q_j}, \quad (\text{A9})$$

defines the generalized nonconservative force associated with the coordinate  $q_j$ . Since the  $q_j$  coordinates are independent and the displacements  $\delta q_j$  are arbitrary, each of the square brackets in Eq. (A8) vanishes, and we therefore obtain Lagrange's equations suitably generalized to include nonconservative forces.

## Appendix B

### DERIVATION OF THE LAGRANGIAN AND GENERALIZED FORCES FOR THE ROCKET PROBLEM

The coordinate variables which can vary independently in the problem are the coordinates  $(r, \phi)$  of the center of mass and the angle of attack  $\alpha$ . Now

$$\mathbf{x}_i = \mathbf{r} + \underline{\rho}_i, \quad (\text{B1})$$

where  $\mathbf{r}$  is the radius vector to the center of mass and  $\underline{\rho}_i$  is the vector displacement from the center of mass to the  $i$ th particle mass element in the rocket. The kinetic energy  $T$  is given by

$$T = \frac{1}{2} \sum_i m_i (\dot{\mathbf{r}} + \dot{\underline{\rho}}_i)^2 = \frac{1}{2} M \dot{\mathbf{r}}^2 + \sum_i \frac{1}{2} m_i \dot{\underline{\rho}}_i^2 + \left( \sum_i m_i \underline{\rho}_i \right) \cdot \dot{\mathbf{r}},$$

but since  $\sum_i m_i \underline{\rho}_i = 0$  by definition of the center of mass, the last term vanishes. Consequently, we have the familiar separation of center of mass motion from internal motion. Now

$$\begin{aligned} \sum_i \frac{1}{2} m_i \dot{\underline{\rho}}_i^2 &= \sum_i \frac{1}{2} m_i [\dot{\underline{\alpha}} \cdot \underline{\rho}_i]^2 = \sum_i \frac{1}{2} m_i \epsilon_{jkl} \dot{\alpha}_k (\rho_i)_l \epsilon_{jmn} \dot{\alpha}_m (\rho_i)_n \\ &= \sum_i \frac{1}{2} m_i (\delta_{km} \delta_{ln} - \delta_{kn} \delta_{lm}) \dot{\alpha}_k \dot{\alpha}_m (\rho_i)_l (\rho_i)_n \\ &= \frac{1}{2} \sum_i m_i [\dot{\alpha}_k \dot{\alpha}_k \rho_{il} \rho_{il} - \dot{\alpha}_k \dot{\alpha}_l \rho_{il} \rho_{lk}] \\ &= \frac{1}{2} \underline{\dot{\alpha}} \cdot \mathbf{I} \cdot \underline{\dot{\alpha}}, \quad \text{where } \mathbf{I} = \sum_i m_i [\rho_i^2 \mathbf{1} - \underline{\rho}_i \underline{\rho}_i]. \end{aligned}$$

In this case of planar motion, where  $\underline{\dot{\alpha}} = \dot{\alpha} \hat{z}$  ( $z$  direction normal to plane),  $\mathbf{I} = \sum_i m_i \rho_i^2$ .

Hence,

$$T = \frac{1}{2} M (\dot{r}^2 + r^2 \dot{\phi}^2) + \frac{1}{2} I \dot{\alpha}^2. \quad (\text{B2})$$

The only conservative force in the problem is gravity, which can be related to a potential:

$$\mathbf{F}_i = -\frac{m_i K}{r_i^2} \hat{r}_i \simeq -\frac{m_i K}{r^2} \hat{r} = \sum_i U_i = -\frac{MK}{r}.$$

Hence, the appropriate Lagrangian which includes conservative forces, is

$$L = \frac{1}{2} M (\dot{r}^2 + r^2 \dot{\phi}^2) + \frac{1}{2} I \dot{\alpha}^2 + \frac{MK}{r} \quad (\text{see Eq. (A7)}). \quad (\text{B3})$$

The nonconservative forces are distributed over the mass elements:

$$\mathbf{L} = \sum_i \mathbf{L}_i, \quad \mathbf{D} = \sum_i \mathbf{D}_i, \quad \mathbf{T} = \sum_i \mathbf{T}_i.$$

From Fig. 2:

$$\begin{aligned} F'_r &= \sum_i (\mathbf{L}_i + \mathbf{D}_i + \mathbf{T}_i) \cdot \frac{\partial}{\partial r} (\mathbf{r} + \boldsymbol{\rho}_i) = (\mathbf{L} + \mathbf{D} + \mathbf{T}) \cdot \hat{\mathbf{r}} \\ &= L \cos \psi - D \sin \psi + T \sin(\psi + \alpha + \beta). \end{aligned} \quad (\text{B4})$$

Similarly,

$$\begin{aligned} F'_\phi &= \sum_i (\mathbf{L}_i + \mathbf{D}_i + \mathbf{T}_i) \cdot \frac{\partial(\mathbf{r} + \boldsymbol{\rho}_i)}{\partial \phi} = (\mathbf{L} + \mathbf{D} + \mathbf{T}) r \cdot \hat{\boldsymbol{\phi}} \\ &= -L \sin \psi - D \cos \psi + T \cos(\psi + \alpha + \beta) r. \end{aligned} \quad (\text{B5})$$

Finally,

$$\begin{aligned} F'_\alpha &= \sum_i (\mathbf{L}_i + \mathbf{K}_i + \mathbf{T}_i) \cdot \frac{\partial}{\partial \alpha} (\mathbf{r} + \boldsymbol{\rho}_i) \\ \delta \boldsymbol{\rho}_i &= 2 \sin \delta\alpha/2 [\hat{\mathbf{z}} \times \boldsymbol{\rho}_i(\alpha)] = \delta\alpha [\hat{\mathbf{z}} \times \boldsymbol{\rho}_i(\alpha)] \\ F'_\alpha &= \sum_i (\mathbf{L}_i + \mathbf{K}_i + \mathbf{T}_i) \cdot [\hat{\mathbf{z}} \times \boldsymbol{\rho}_i]. \end{aligned}$$

Now we use the information that lift and drag act as if concentrated at the center of pressure and thrust acts as if localized at the center of combustion:

$$F'_\alpha = (\mathbf{L} + \mathbf{D}) \cdot (\hat{\mathbf{z}} \times \mathbf{l}_2) + \mathbf{T} \cdot (\hat{\mathbf{z}} \times \mathbf{l}_1) = l_2 [L \cos \alpha + D \sin \alpha] - l_1 T \sin \beta. \quad (\text{B6})$$

## Appendix C

### VELOCITY INCREMENT ESTIMATES FOR VARIOUS EFFECTS IN FIRST-STAGE ROCKET MOTION

The ideal velocity (i.e., from thrust only) of a large rocket at first-stage cutoff [1-3] could be estimated (e.g., see Eq. (8) of text) as

$$\Delta v_T = \int_0^{t_1} (T/M) dt \approx (T/\bar{M}) t_1, \quad (C1)$$

where  $t_1$  is the burn duration of the first stage, and  $\bar{M}$  is an average mass. The gravity loss from this velocity is

$$\Delta v_G \approx g t_1 \approx 0.3(T/\bar{M}) t_1, \quad (C2)$$

where we indicate a 30% gravity loss [2]. Now  $\Delta v_T$  might be  $\approx 3050$  m/s, so that  $\Delta v_G \approx 900$  m/s. The drag loss from  $\Delta v_T$  is probably  $\approx 5\%$  overall, although the drag force can reach a maximum of about 25% of the thrust force during the first-stage motion [2].

Hence,

$$\Delta v_D \approx 150 \text{ m/s} \approx 0.05 \Delta v_T, \quad (C3)$$

which is almost canceled by thrust increase due to ambient pressure decrease in the ascent [2,3]. By comparison we have a relatively large value [5] of velocity imparted by earth's rotation

$$v_o \approx \omega_E R = 450 \text{ m/s} \approx 0.15 \Delta v_T. \quad (C4)$$

We estimate the Coriolis effect as

$$\Delta v_{Cor} \approx \int_0^{t_1} 2\omega_E v dt \approx 2\omega_E (T/\bar{M}) \int_0^{t_1} t dt$$

or

$$\Delta v_{Cor} \approx \omega_E t_1 \Delta v_T \approx 0.01 \Delta v_T \quad (C5)$$

for a burn time  $t_1$  somewhat more than 2 min. The centrifugal effect contribution is given as

$$\Delta v_{cent} \approx \omega_E^2 R t_1 \approx \omega_E t_1 v_o \approx 0.0015 \Delta v_T. \quad (C6)$$

## Appendix D

### DETERMINATION OF LAUNCH PROFILE PARAMETERS FROM DESIRED ORBIT INJECTION CONDITIONS IN A FLAT EARTH APPROXIMATION

If we are given a set of desired orbit injection conditions, such as altitude  $y$ , rocket speed  $v$ , heading  $\psi$ , and azimuth angle  $a$ , we face the question of the launch profile conditions needed to obtain them. We design the rocket to attain the speed  $v'$  and  $y'$  at burnout (disregarding earth's rotation) for a final heading  $\psi'$ , and need to determine the apparent launch azimuth  $a_0$ . The relationship between these parameters is obtained with the help of the vector diagram in Fig. D1. The notation used here has been defined in Section 3 of the text (cf. also Figs. 4 and 6). The following results may readily be obtained.

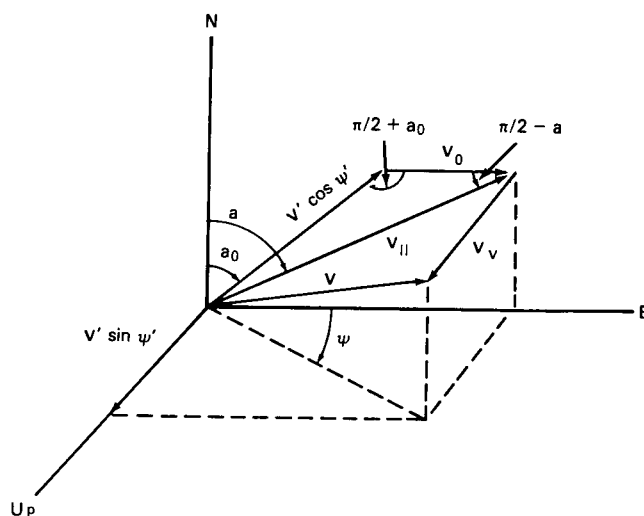


Fig. D1 — Vector diagram for determination of launch profile parameters from desired orbit injection conditions (flat earth approximation)

$$\begin{aligned} v' &= |\mathbf{v} - \mathbf{v}_0| = |\mathbf{v}_v + \mathbf{v}_H - \mathbf{v}_0| = \{v_v^2 + (v_{||} - v_0)^2\}^{1/2} \\ &= \{v^2 - 2vv_0 \cos \psi \sin a + v_0^2\}^{1/2}. \end{aligned} \tag{D1}$$

With  $v'$  thus determined, we use the following from Fig. D1:

$$\sin \psi' = v \sin \psi / v'. \tag{D2}$$

This determines  $\psi'$ , and now if we define

$$\Delta a = a - a_0 \tag{D3}$$

and use the law of sines in Fig. D1,

$$\sin \Delta a = v_0 \cos a / (v' \cos \psi'), \tag{D4}$$

from which  $a_0$  is determined. Since  $v_0$  is in the horizontal plane, we have

$$y' = y. \tag{D4}$$

A similar set of equations has been derived by Ruppe [3].

## Appendix E

### THRUST INCREASE AND AERODYNAMIC EFFECTS

For a rocket with swivel control motors the total thrust includes pressure forces and is normally presented [2,3,6] as

$$T = \dot{M}v_e + A[p_e - p(y)], \quad (\text{E1})$$

where  $\dot{M}$  is the mass loss rate of exhaust gases,  $v_e$  is the actual average axial speed of these gases relative to the rocket,  $A$  is the exit aperture area,  $p_e$  is the pressure of the exhaust gases at the exit aperture, and  $p(y)$  is the ambient pressure of the atmosphere at altitude  $y$ . Normally,  $p(y)$  varies from  $p(o)$  to zero for first-stage motion, so that the thrust varies from its sea level value  $T_{s1}$  to its vacuum value  $T_{vac}$ . Hence,  $T_{s1}$  and  $T_{vac}$  are usually given for the first stage, and  $T_{vac}$  is given for the higher stages of a rocket. In effect the ratio

$$x \equiv T_{vac}/T_{s1} \quad (\text{E2})$$

is given for the first-stage motion, and it is easily shown that (E1) can be rewritten as

$$T = T_{vac} \left[ 1 - \frac{x-1}{x} \frac{p(y)}{p(o)} \right]. \quad (\text{E3})$$

Very frequently  $x$  is the range 1.12 to 1.15, and the increase of thrust with altitude is thus exhibited.

As we have indicated in the text, drag tends to counterbalance the effect of thrust increase. The aerodynamic forces of lift  $L$  and drag  $D$  are important in first-stage motion, where angles of attack  $\alpha$  are normally programmed to be small (e.g.,  $\alpha \approx 3^\circ$ ). From [2] one then has for the aerodynamic forces:

$$D = [C_{DO} + C_{DL} \alpha^2] (\rho v^2/2) S$$

$$L = [\partial C_L/\partial \alpha] \alpha (\rho v^2/2) S, \quad (\text{E4})$$

where  $\rho$  is the atmospheric density,  $v$  is the rocket speed, and  $S$  is an appropriate reference cross-sectional area (e.g., that for the first stage) to which the aerodynamic coefficients are referred. These coefficients for a two-stage rocket are shown by Ehrlicke [2] in his Fig. 5-8 as a function of local mach number, which is the speed  $v$  divided by the speed of sound at the altitude of the rocket. One may thus infer the aerodynamic forces from standard atmosphere data and the aerodynamic coefficients.